



This item was submitted to Loughborough's Institutional Repository (<https://dspace.lboro.ac.uk/>) by the author and is made available under the following Creative Commons Licence conditions.

The image shows a yellow rectangular box containing the Creative Commons Attribution-NonCommercial-NoDerivs 2.5 license summary. At the top is the Creative Commons logo (CC) and the text 'creative commons' in a bold, lowercase font, with 'COMMONS DEED' in a smaller, spaced-out font below it. The license title 'Attribution-NonCommercial-NoDerivs 2.5' is centered. Below this, the text 'You are free:' is followed by a bullet point: 'to copy, distribute, display, and perform the work'. Then, 'Under the following conditions:' is followed by three items, each with a circular icon: 1. 'BY: Attribution' with a person icon, stating 'You must attribute the work in the manner specified by the author or licensor.' 2. 'Noncommercial' with a dollar sign and a slash icon, stating 'You may not use this work for commercial purposes.' 3. 'No Derivative Works' with an equals sign icon, stating 'You may not alter, transform, or build upon this work.' Below these are two more bullet points: 'For any reuse or distribution, you must make clear to others the license terms of this work.' and 'Any of these conditions can be waived if you get permission from the copyright holder.' At the bottom, it states 'Your fair use and other rights are in no way affected by the above.' and 'This is a human-readable summary of the [Legal Code \(the full license\)](#).' A 'Disclaimer' link with a document icon is at the very bottom.

**CC creative commons**  
COMMONS DEED

**Attribution-NonCommercial-NoDerivs 2.5**

**You are free:**

- to copy, distribute, display, and perform the work

**Under the following conditions:**

**BY:** **Attribution.** You must attribute the work in the manner specified by the author or licensor.

**Noncommercial.** You may not use this work for commercial purposes.

**No Derivative Works.** You may not alter, transform, or build upon this work.

- For any reuse or distribution, you must make clear to others the license terms of this work.
- Any of these conditions can be waived if you get permission from the copyright holder.

**Your fair use and other rights are in no way affected by the above.**

This is a human-readable summary of the [Legal Code \(the full license\)](#).

[Disclaimer](#)

For the full text of this licence, please go to:  
<http://creativecommons.org/licenses/by-nc-nd/2.5/>

## CHARACTERISATION OF LASER SCRIBES IN THIN FILM PHOTOVOLTAICS BY COHERENCE CORRELATION INTERFEROMETRY

B. Maniscalco<sup>1</sup>, P. M. Kaminski<sup>1</sup>, G. Claudio<sup>1</sup>, J.M. Walls<sup>1</sup>  
 Y. Yu<sup>2</sup>, D. Mansfield<sup>2</sup>  
 M. Crozier<sup>3</sup>, A. Brunton<sup>3</sup>

<sup>1</sup>Centre for Renewable Energy Systems Technology, (CREST), School of Electronic, Electrical and Systems Engineering, Loughborough University, Leicestershire, LE11 3TU, UK

<sup>2</sup>Taylor Hobson Ltd, AMETEK Ultra Precision Technologies, PO Box 36, 2 New Star Road, Leicester, LE4 9JG, UK

<sup>3</sup>M-Solv Ltd, Oxonian Park, Langford Locks, Kidlington, OX5 1FP, UK

**ABSTRACT:** In this paper we present results measuring the precise shape of laser scribes in thin film photovoltaics using Coherence Correlation Interferometry (CCI). Laser ablation is used in interconnect processes in all types of thin film devices, including those based on CdTe, CIGS and amorphous silicon. The work presented in this paper was focused on the use of a laser ablation process in the interconnect of thin film CdTe modules. This process is known as monolithic integration. The laser scribe measurements presented here were obtained on a nanometre scale using Coherence Correlation Interferometry. The Coherence Scanning Interferometry (CSI) technique is able to provide three and two dimensional topographical images of the sample surface, with an ultimate vertical resolution of 0.01nm. It provides two dimensional profiles of the laser ablated trenches, from which it is possible to extract quantitative information of the detailed shape of the scribe including precise measurements of both depth and width. In addition, the CCI is able to provide detailed analysis of surface roughness within the bottom of the trench which is important for efficient electrical contact.

**Keywords:** CdTe, Laser Processing, Module Integration, Surface metrology

### 1 INTRODUCTION

In recent years there has been considerable interest in thin film photovoltaics [1]. Cadmium telluride solar cells are to date the most commercially successful thin film PV. The devices are multi-layer semiconductor systems deposited on glass in a superstrate configuration. A Transparent Conducting Oxide (TCO) is used as a front contact, Cadmium Sulphide (CdS) is used as a window layer and Cadmium Telluride (CdTe) is the absorber layer. A p-n junction is formed at the interface between CdS and CdTe [2]. In contrast to Silicon-based photovoltaics, these devices are manufactured as modules and not as single cells. The current output from the whole module is too high to be used directly, so it is necessary to divide the module into different cells and connect them in series. There are different methods to isolate the PV cells, involving mechanical or laser scribing. In this paper, we report on the measurement of scribes in thin film photovoltaic devices produced using laser ablation. The standard procedure involves three steps, with an initial scribe down to the glass which divides the conductive coating on the glass into isolated stripes, then thin film deposition occurs (CdS and CdTe), followed by post-deposition treatments (CdCl<sub>2</sub> and annealing) and the module is scribed again, and the back contact is deposited. In the final scribe after contact is formed cells are isolated within the module. The second scribe, performed after deposition of the semiconductor layer, provides the interconnect path. The third scribe cuts the top electrode down to the TCO layer to isolate the cells and complete the fabrication into a series-interconnected structure. This pattern is then repeated equally spaced in the module [3]. It is important for the interconnect to have low series and high shunt resistance. Residual material in the trenches, from both semiconductor layers and the TCO, can cause resistance problems. Shunting derives from possible bridging material left at the end of the interconnection process. Laser scribe measurement is important in order to assess the process. The trenches

have to be precise in depth, especially down to the TCO, which is only about 300nm in thickness. If the laser cuts to the wrong position reaching either the semiconductor layer or cutting into the TCO the contact resistance of the interconnect will be affected or no connection will be achieved.

### 2 METHOD

#### 2.1 Coherence Correlation Interferometry

There are many techniques used for the metrology of surface finish. Coherence Scanning Interferometry (CSI) is an important tool since it is non-contacting and hence a non-destructive technique. In this work, we used a variant of CSI, a "SunStar" Coherence Correlation Interferometer (CCI) from Taylor Hobson Ltd [4]. The CCI combines a coherence correlation algorithm with a high-resolution digital camera array to generate a three-dimensional representation of a structure by scanning the fringes through the surface and then processing the information to transform the data into a quantitative three-dimensional image with 0.01nm vertical resolution. It uses a white light source, which produces a beam which is split into two components, one act as a reference optical path and the other scans the surface. Recently, the technique has been also extended to measurements of thin film thickness from semi-transparent materials [5,6]. The advantage of CCI over other metrology techniques such as the AFM is that it takes its data from a relatively large and hence more representative area. The lateral resolution can reach ~0.3µm and is determined by the wavelength of light and the numerical aperture (NA) of the objective lens. CCI provides both three dimensional topographical images and two dimensional profiles, from which accurate quantitative data can be extracted. It provides surface morphology characterisation, with analysis of surface roughness. Standard parameters, such as RMS roughness (Sq), maximum peak and valley height (St and Sv) and arithmetical mean roughness (Sa) can be extracted quickly.

The analysis area was scanned using the 'stepped and smooth' mode, provided in the CCI operational software. Depending on the magnification of the lens (10x, 20x, 50x), different fields of view were captured by the CCD camera array, corresponding to areas 1.65mm x 1.65mm, 825 $\mu$ m x 825 $\mu$ m and 330 $\mu$ m x 330 $\mu$ m. This allows the analysis of more features in the same field of view, with a lower resolution (10x and 20x) or detailed analysis of a single feature, with high resolution (50x). Once the image was captured, it was processed using 'Talymap' software provided by Taylor Hobson, which allows three dimensional images of the laser scribes to be created, enlarging the z-axis, so that it is possible to have a clear visualization of the trench shape. Two-dimensional profiles were extracted from the image and a quantitative analysis including 'step-height' and 'horizontal difference' obtained. A variety of laser scribing parameters have been varied to discover the optimum conditions on various types of cell. Each one was characterised with CCI; both depth and width were studied, together with surface texture at the bottom of the scribe in order to check the trench smoothness. It is important to obtain a smooth edge to the scribe and as smooth a surface as possible at the bottom of the scribe.

## 2.2 Laser scribing

Measurements were obtained for samples prepared using different laser operating parameters during the ablation process. In this paper, we present some examples from this optimisation process, involving different laser powers, different focus conditions and different shot overlaps. Each single scribe has to be analysed and the main parameters to be checked are: dimensions (width and depth), surface form (humps) and roughness at the bottom of the scribe. Single scribes were ablated on glass/FTO/CdS/CdTe samples and the width and depth were measured with the goal of optimising the P2 scribe. These parameters are characteristic for each type of sample, depending on the thickness of each layer of the multi-stack device. Thickness depends on the deposition methods and post-deposition treatments, which can vary according to the manufacturer. It is then necessary to optimise the laser parameters to obtain the desired results.

## 3 EXPERIMENTAL RESULTS

Thin film CdTe solar cells were scribed using an Nd:YAG laser with a wavelength of 532nm (Spectra Physics Explorer-532-2Y) from the glass side. Parameters such as focus, pulse energy and frequency were investigated to test their influence on the trench formation. Depth and width of the scribe were monitored as the most important parameters for the interconnect process using x50 lens, the field of view was 330 $\mu$ m x 330 $\mu$ m with ~0.4 $\mu$ m lateral resolution. Debris formation was checked since its presence could have a negative effect on the module efficiency.

### 3.1 Laser power

The first parameter which was varied in the process was the laser power, controlled by the pulse energy which was varied in range from 80  $\mu$ J to 4  $\mu$ J.

From 80 to 50 $\mu$ J, the laser power was too high and resulted in a very rough bottom of the scribe, at this pulse energy the laser scribe penetrated too deep into the stack. This is shown in figure 1, for 80 $\mu$ J and 75 $\mu$ J pulse

energy.

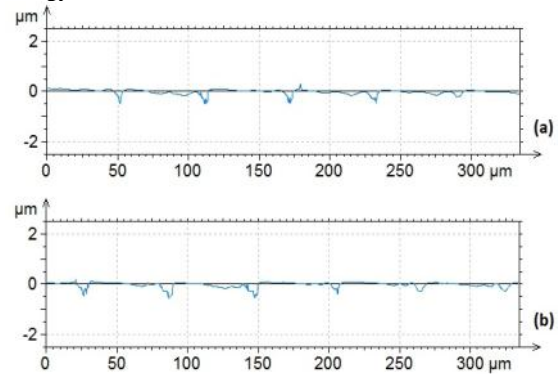


**Figure 1:** Two dimensional CCI profiles of scribes obtained using a) 80 $\mu$ J and b) 75 $\mu$ J pulse energy at 5kHz showing damage to the substrate.

Decreasing the laser power made the scribes smoother. At 44 $\mu$ J and especially at 33 $\mu$ J, the bottom appears to be really smooth and the shape and dimensions meet the requirement for the interconnect process. Figure 2 shows, the full analysis of the scribe obtained at a pulse energy of 33 $\mu$ J.

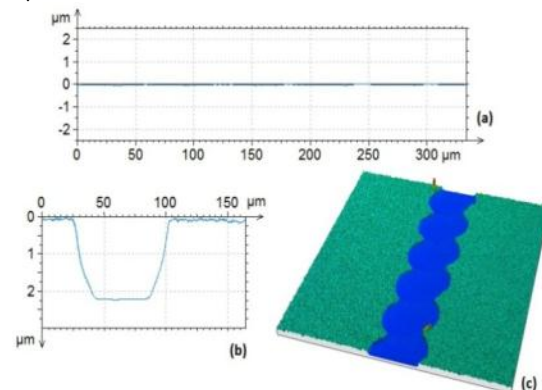


**Figure 2:** a) 2D CCI profile along the scribe, b) 2D cross-sectional CCI profile and c) 3D topographical CCI image of laser scribe obtained at 33 $\mu$ J pulse energy, optimum focus and 5 kHz frequency.

From 24 $\mu$ J to 4  $\mu$ J, the pulse energy is below the ablation threshold therefore the material is not affected by the laser.

The optimum scribe was obtained by just varying the laser power parameter used the following conditions: 5kHz frequency at 300mm/s stage speed and 35 $\mu$ J pulse energy. Further improvements could be obtained by adjusting the laser focus.

### 3.2 Laser focus

The lens is on a moveable z-stage and at a certain distance the mask is positioned at the image plane of the lens. Using this setting, an image of the mask on the work piece is obtained with relatively uniform energy density.

The focus was varied in order to optimize the shape of the scribes. The position of the lens was varied  $\pm$ 2mm with 0.1mm resolution. At the focus the bottom of the scribe is uniform and no damage to the glass is made. Observing the cross section of the bottom of the scribe allows characterization and control of the debris

formation.

Figure 3 shows the cross section along the scribes for various laser focus values. The two-dimensional profiles were obtained using Coherence Correlation Interferometry (CCI). This instrument provides both two and three dimensional topographical images of the surface. Profiles both along the scribe and as cross-section can be easily obtained from the three dimensional image.

The profiles show how changing the focus by +0.3mm, influences the profile of the scribe and the debris formation. This effect is mainly due to the re-melting of the material during the scribing process. At the optimal focal point, the scribe looks smoother along the scribe; however decreasing the focus to -0.3mm increases roughness along the scribe.

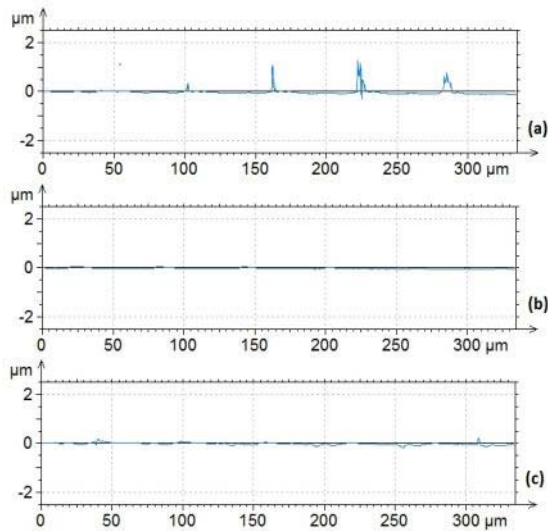


**Figure 3:** Two dimensional CCI profiles of the bottom of the scribe along the scribe of a) +0.3mm focus, b) lens at focus and c) -0.3mm focus.

In both Figure 4(a) and 4(b), the scribe obtained at optimal working distance appears smooth and well-shaped. In the three dimensional image, which shows the scribe appearance, the laser shots can be clearly identified with a characteristic round shape; the scribe was continuous and no significant effect on the final performance should occur.

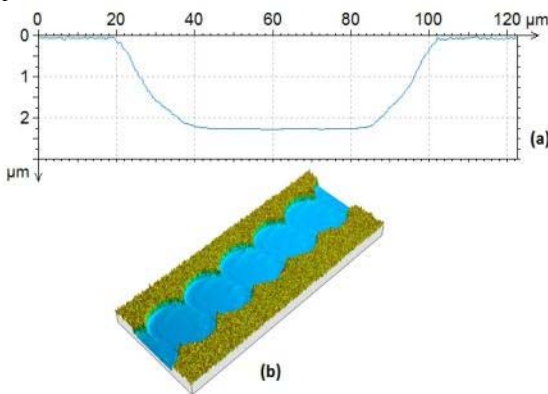


**Figure 4:** a) Three dimensional topographical CCI image and b) two dimensional cross-sectional CCI profile of the optimal working distance scribe.

The optimized combination of laser parameters were found to be: frequency 5 kHz at stage speed of 300mm/s

and pulse energy 35μJ. Pulse frequency and laser power were also varied simultaneously, this can allow an increase in the scribe speed and a shortening of the process.

### 3.3 Pulse frequency and laser power

Another parameter which was changed in the process is the pulse frequency. In the previous cases, the pulse frequency was kept constant at 5 kHz, changing the pulse frequency allows the pulse overlap to be controlled. The diode current can be simultaneously changed, in order to maintain the optimum pulse energy and therefore appropriate scribe shape.

The frequency was varied in range from 2 kHz to 50 kHz. Pulse energy was kept constant at 35μJ, up to 30kHz where it is limited by the peak power of the laser to 23 μJ and 13 μJ at 50kHz.

Up to 5 kHz, a continuous scribe was not obtained. Individual dots appeared on the surface formed by individual laser pulses. The pulse frequency was too low to obtain overlap at the stage speed of 300mm/s, so that each crater represents an individual laser shot. The space between them is determined by the frequency used as the stage speed was kept constant. Figure 5 shows scribes obtained at 2 kHz and 3 kHz.

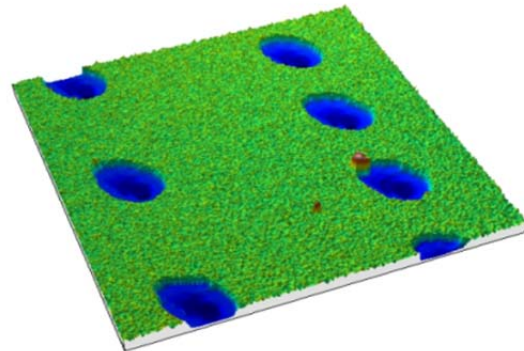


**Figure 5:** 2 kHz(left) and 3 kHz(right) laser scribes.

Further increasing the pulse frequency, beyond the optimized value of 5 kHz, leads to an increase in power density and results in excessive scribe depth and deformation of the shape. The dimensions for the optimized scribe were: 2.22μm deep and 83.8μm wide. Increasing the frequency leads to deeper and narrower scribe formation. Figure 6 shows the two dimensional cross sectional profiles obtained with CCI. The shape is distorted as the frequency is increased.

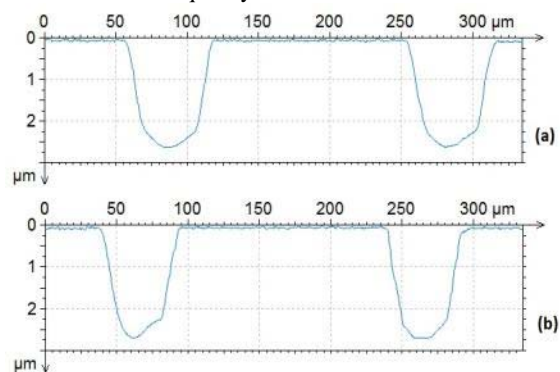


**Figure 6:** Two dimensional cross sectional CCI profiles of a) 10 kHz b) 11 kHz c) 40 kHz d) 50 kHz.

In figure 6, the depths and widths of the scribes are respectively: a) 2.45 $\mu\text{m}$  and 63.5 $\mu\text{m}$ , b) 2.47 $\mu\text{m}$  and 62.4 $\mu\text{m}$ , c) 2.49 $\mu\text{m}$  and 54.6 $\mu\text{m}$ , d) 2.58 $\mu\text{m}$  and 53.1 $\mu\text{m}$ .

As the pulse frequency increased the bottom of the scribe appeared to be smoother, although the shape was deteriorating. Figure 7 shows a comparison between the 10 kHz and the 50 kHz scribes.

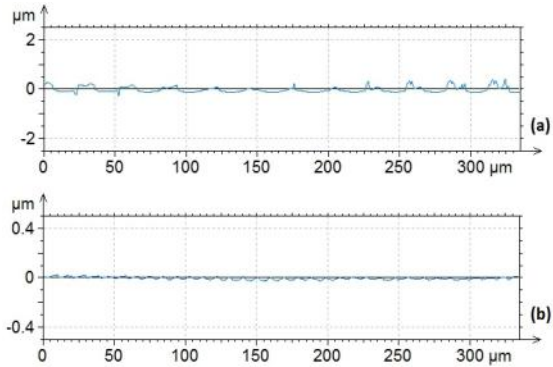


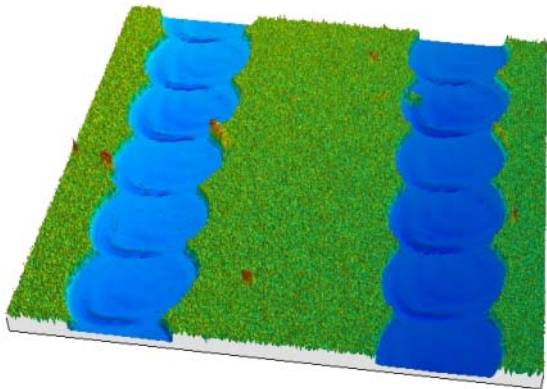
**Figure 7.** Two dimensional CCI profiles of a) 10 kHz and b) 50 kHz scribes.

### 3.4 Control of debris formation

Debris formation can occur and is associated with both pulse energy and the quality of the focus level. If these values are not optimized then excessive debris will be formed. This can lead to shunting problems during the interconnecting process.

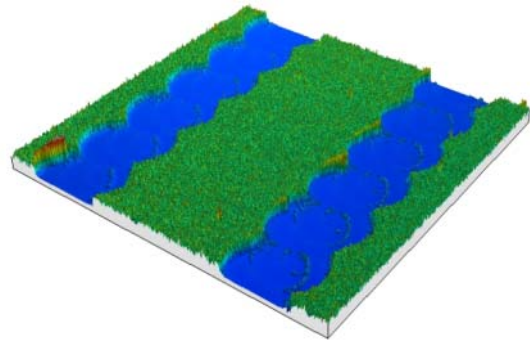
Debris is formed for high pulse energies: from 80 to 44 $\mu\text{J}$ . while, at 33 $\mu\text{J}$ , the scribe looks smooth and free from debris formation. For values lower than 33 $\mu\text{J}$ , the pulse energy is not sufficient to scribe the material.

Figure 8 shows a three dimensional image of two scribes obtained at high pulse frequency (80 $\mu\text{J}$  and 75 $\mu\text{J}$ ). The laser shots can be easily identified and it is possible to see where material has been melted and recast at the overlap of each subsequent pulse..



**Figure 8.** Three dimensional images of two scribes obtained at 5 kHz frequency. The pulse energy was 80 $\mu\text{J}$  for the right scribe and 75 $\mu\text{J}$  for the left one.

High debris formation occurs as the focus is changed. For + 0.3 and +0.2 mm from the optimum focus point, the scribes show high debris formation around the laser shots, due to incomplete material removal, which is visible in both cases. This effect decreased as the optimum working distance is reached and is symmetrical about the focal point



**Figure 9.** Three dimensional image of two scribes obtained at 5 kHz frequency, at +0.3mm from the optimum focus for the right scribe and at +0.2mm for the left one.

## 5 CONCLUSIONS

Thin film CdTe solar cells were scribed using a frequency doubled Nd:YAG laser to form the structures required for monolithic series interconnection. The scribes were characterised using CCI, which provided 3D maps of the surface and 2D scribe profiles. It was used to monitor the shape and dimensions of the scribe as well as the formation of debris during the process.

Various parameters were changed in order to optimize the laser processing. Debris formation was monitored as it is important to obtain a well-shaped scribe without debris formation both at the bottom and at the edges for correct interconnect. The depth control of the scribe is important because depending on the type of the scribe (P1, P2 or P3), either the TCO or the glass layer has to be reached and any errors lead to a decrease in module performance. If the scribe does not penetrate to the right layer, shunting problems are likely to occur. The width also has to be controlled since it defines the contact resistance and the shaded area of the module.

Pulse energy has to be precisely controlled since if it is too low the material is not completely removed. On the other hand use of too high a pulse energy forms scribes that are too deep, damages the underlying layer causing increased roughness and producing excess debris. Similar effects occur when the pulse frequency is increased.

Correct focus of the laser was found to be very important for debris formation. Defocusing of the laser leads to incomplete material removal and debris formation at the bottom of the scribe.

## 4 REFERENCES

- [1] L D. Partain, LM. Fraas 'Solar Cells and Their Applications', *John Wiley and Sons, Technology & Engineering*, 2010.
- [2] Robert Triboulet, Paul Siffert, 'CdTe and Related Compounds', *Elsevier, Technology & Engineering*, 2009.
- [3] B A Korevaar et al., 'Monolithically integrated solar modules and methods of manufacture', US 2010/0236607 A1, 2010.
- [4] A Bankhead and I McDonnell, 'Interferometric Surface Profiling', GB2390676, 2004
- [5] D Mansfield, "The distorted helix: thin film extraction from scanning white light interferometry", *Proc. SPIE* vol.6186, 2006
- [6] D Mansfield, "Extraction of film interface surfaces from scanning white light Interferometry", *Proc. SPIE* vol. 7101, 2008